Design of Sliding Mode Controller for the 2D Motion of an Overhead Crane with Varying Cable Length

Le Anh Tuan
Department of Mechanical Engineering, Vietnam Maritime University, Vietnam
Email: tuanla.ck@vimaru.edu.vn

***Abstract*—Overhead cranes are under-actuated systems. They have three outputs that need to be controlled, consisting of cargo swing angle, trolley displacement, and suspended cable length, but only two actuators: cargo lifting and trolley driving forces. The main objective of this study is to design a robust controller for an overhead crane that transfers cargo from point to point as fast as possible and, at the same time, keeps the cargo swing angle small during the transfer process and make it completely vanish at the desired cargo destination. The proposed controller must simultaneously carry out three duties: minimize cargo swing, track trolley to the desired destination, and lift/lower cargo to the reference length of cable. The controller is designed based on a sliding mode control technique. To validate the proposed control quality, a stability analysis of the system is discussed and the response analysis is executed with both MATLAB simulation and experimental research. The simulation and experiment results show that the crane system is stable and has the desired behavior.**

***Index Terms*—Lyapunov function, overhead cranes, sliding mode control, switching suface, under-actuated systems**

I. Introduction

Overhead cranes are widely used in many different industrial fields such as shipyards, automotive factories, and other industrial factories. To increase productivity, many types of cranes are required in fast operation. This means the time cycle of cargo transport must be short. The fast operation of overhead cranes without control leads to cargo swing on wire rope - the faster the cargo transport, the larger the cargo swing angle. This results in a dangerous situation during the operation process; it is possible to damage the factory, the crane, and other equipment. More seriously, it may cause accidents if the cargo swing angle is too large.

Papers on the control of overhead crane could be divided into two groups: control of two-dimensional (2D) overhead crane and three-dimensional (3D) overhead crane. Many crane control techniques are also available. Some authors concentrate on crane nonlinear control [1]-[3]. Many researchers recently focused on intelligent control approaches of cranes such as fuzzy logic [4], [5], neural network control [6], and so on.

The robust control of cranes, especially structure variable control (SVC) technique, has been studied by many researchers. Lee [7] suggested a sliding mode anti-swing control for overhead cranes designed based on Lyapunov stability theorem. Shyu [8], [9] presented a sliding mode control (SMC) to minimize swing angle and maximize trolley speed. Almutairi [10] dealt with SMC for 3D overhead crane using a fully dynamic model including five nonlinear second order differential equations. His study proposed an observer to estimate immeasurable states of 3D crane system. Liu [11] considered an adaptive sliding mode fuzzy control approach for overhead cranes in case of combination of trolley moving and bridge traveling. However, the cargo suspended cable is viewed as a constant length element. The works [8]-[10] only achieve the simulation results without experiment. Motivated by [8]-[11], we propose the sliding mode controller for overhead crane in which the variation of cargo lifted cable is taken into account. And, both theoretical and experimental results are shown in our study.

The SMC approach is classified as a variable structure control technique with many advantages. It is known to be robust, easy to implement, and insensitive to uncertainties and disturbance [12]. Its robustness is due to a natural capability to deal with uncertain objects. It is especially suitable for under-actuated systems with uncertainties. 2D overhead cranes are under-actuated systems in which cargo mass is considered uncertain. They have three output variables that need to be controlled (cargo swing angle, trolley displacement, and cable length) and only two control inputs (trolley moving and cargo lifting forces). Therefore, the SMC technique is a proper selection in this case. Furthermore, cargo swing is directly concerned with trolley motion and length of cable. Thus, simultaneously combining the control of these output variables is not easy to implement and needs proper control actions. In this article, we propose a new robust controller for 2D overhead cranes based on the SMC technique. The proposed controller concurrently

Manuscript received August 24, 2014; accepted June 3, 2015.
This research is funded by the Vietnam National Foundation for Science and Technology Development (NAFOSTED) under grant number 107.01-2013.04.

©2016 Journal of Automation and Control Engineering

doi: 10.18178/joace.4.3.181-188

executes three duties consisting of vanishing cargo swing, tracking trolley, and lifting/lowering cargo to desired positions. The suggested controller stabilizes the crane system and guarantees convergence of system responses to desired values.

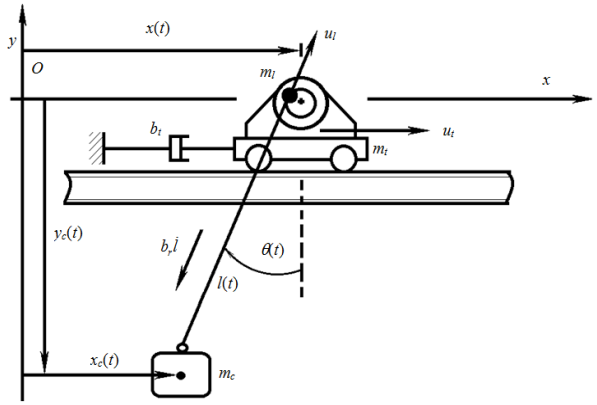

Figure 1. Physical modeling of 2D overhead crane

This paper is organized as follows. In Section 2, we establish a physical model, a fully nonlinear mathematical model of 2D overhead crane, and its compact form. Section 3 presents the design of a sliding mode controller including switching surface selection and SMC scheme design. System stability analysis is shown in Section 4. Simulation of system responses, experimental study, and results analysis are given in Section 5. Finally, some concluding remarks are presented in Section 6.

II. System Dynamics

In this section, we build a dynamic model of an overhead crane that simultaneously combines trolley and cargo lifting motions. A physical model is given in Fig. 1. The dynamic system has three masses composed of m_t, m_c, and m_l. The cargo mass m_c and trolley mass m_t are considered point masses concentrated at their centers. m_l denotes equivalent mass of all rotating components of the cargo lifting mechanism. Chosen generalized coordinates of the system include $x(t)$, $l(t)$, and $\theta(t)$, namely, trolley displacement, cable length, and cargo swing angle, respectively. Furthermore, frictions of trolley moving and cargo hoisting are respectively characterized by b_t and b_r. Forces of driving motors of trolley travelling and cargo lifting u_t, u_l, are created so that the trolley moves and handles cargo from the starting point to its destination as fast as possible and at the same time, minimizes the cargo swing.

For convenience, the following assumptions are given. (i) The mass and elastics of wire rope are neglected. (ii) There is no effect of disturbance caused by wind outside the factory floor since the overhead crane usually works indoors. (iii) The motions of all components of system are considered in a plane.

By using virtual work principle and Lagrange's equation, we can derive the motion equations describing the system dynamics as follows

$$\begin{pmatrix} (m_t+m_c)\ddot{x}-m_c\sin\theta\ddot{l}-m_c l\cos\theta\ddot{\theta} \\ +b_t\dot{x}-2m_c\cos\theta\dot{l}\dot{\theta}+m_c l\sin\theta\dot{\theta}^2 \end{pmatrix}=u_t(t) \tag{1}$$

$$\begin{pmatrix} -m_c\sin\theta\ddot{x}+(m_c+m_l)\ddot{l} \\ +b_r\dot{l}-m_c l\dot{\theta}^2-m_c g\cos\theta \end{pmatrix}=u_l(t) \tag{2}$$

$$-\cos\theta\ddot{x}+l\ddot{\theta}+2\dot{l}\dot{\theta}+g\sin\theta=0 \tag{3}$$

The system dynamics including Equations (1), (2), and (3) can be rewritten in the matrix form

$$\mathbf{M}(\mathbf{q})\ddot{\mathbf{q}}+\mathbf{C}(\mathbf{q},\dot{\mathbf{q}})\dot{\mathbf{q}}+\mathbf{G}(\mathbf{q})=\mathbf{F} \tag{4}$$

where, $\mathbf{M}(\mathbf{q})=\mathbf{M}^T(\mathbf{q})$ is symmetric mass matrix. $\mathbf{C}(\mathbf{q},\dot{\mathbf{q}})$ denotes damping and centrifugal matrix. $\mathbf{G}(\mathbf{q})$ is a matrix of gravity. $\mathbf{F}$ denotes a matrix of control forces of driving motors. These matrices are determined as follows

$$\mathbf{M}(\mathbf{q})=\begin{bmatrix} m_{11} & m_{12} & m_{13} \\ m_{21} & m_{22} & 0 \\ m_{31} & 0 & m_{33} \end{bmatrix};\ \mathbf{C}(\mathbf{q},\dot{\mathbf{q}})=\begin{bmatrix} c_{11} & c_{12} & c_{13} \\ 0 & c_{22} & c_{23} \\ 0 & c_{32} & c_{33} \end{bmatrix};$$

$$\mathbf{F}=\begin{bmatrix} u_t \\ u_l \\ 0 \end{bmatrix};\ \mathbf{G}(\mathbf{q})=\begin{bmatrix} 0 \\ g_2 \\ g_3 \end{bmatrix};\ \mathbf{q}=\begin{bmatrix} x \\ l \\ \theta \end{bmatrix};$$

The coefficients of $\mathbf{M}(\mathbf{q})$ matrix are given by

$$m_{11}=m_t+m_c;\ m_{12}=-m_c\sin\theta;\ m_{13}=-m_c l\cos\theta;$$
$$m_{21}=-m_c s\sin\theta;\ m_{22}=m_c+m_l;\ m_{31}=-m_c l\cos\theta;$$
$$m_{33}=m_c l^2;$$

The coefficients of $\mathbf{C}(\mathbf{q},\dot{\mathbf{q}})$ matrix are determined by

$$c_{11}=b_t;\ c_{12}=-m_c\cos\theta\dot{\theta};\ c_{13}=m_c l\sin\theta\dot{\theta}-m_c\cos\theta\dot{l};$$
$$c_{22}=b_r;\ c_{23}=-m_c l\dot{\theta};\ c_{32}=m_c l\dot{\theta};\ c_{33}=m_c l\dot{l};$$

The nonzero coefficients of $\mathbf{G}(\mathbf{q})$ vector are given by

$$g_2=-m_c g\cos\theta;\ g_3=m_c lg\sin\theta;$$

An overhead crane is an under-actuated system. The system has three controlled outputs but only two actuators, u_t and u_l. Therefore, we separate the mathematical model of the crane into two auxiliary system dynamics: un-actuated and actuated mathematical models. Similarly, three generalized coordinates need to be separated: $\mathbf{q}_1=\begin{bmatrix} x & l \end{bmatrix}^T$ for actuated and θ for un-actuated dynamics. To determine the un-actuated state θ, we can rewrite dynamics (3) as follows

$$\ddot{\theta}=\frac{1}{l}\left(\cos\theta\ddot{x}-2\dot{\theta}\dot{l}-g\sin\theta\right) \tag{5}$$

From the previous equation, we can realize that the cargo swing angle θ is directly affected by properties of the trolley motion x and the length of wire rope l. Substituting (5) into (1) and combining with (2), we obtain the following actuated mathematical model

$$\begin{pmatrix} \left(m_t + m_c - m_c \cos^2\theta\right)\ddot{x} - m_c \sin\theta \ddot{l} \\ +b_t \dot{x} + m_c l \sin\theta\dot{\theta}\dot{\theta} + m_c g \sin\theta\cos\theta \end{pmatrix} = u_t(t) \quad (6)$$

$$\begin{pmatrix} -m_c s\sin\theta\ddot{x} + \left(m_c + m_l\right)\ddot{l} + b_r \dot{l} \\ -m_c l\dot{\theta}\dot{\theta} - m_c g\cos\theta \end{pmatrix} = u_l(t) \quad (7)$$

The previous actuated dynamics can be rewritten in matrix equation form

$$\bar{\mathbf{M}}(\mathbf{q})\ddot{\mathbf{q}}_1 + \mathbf{B}\dot{\mathbf{q}}_1 + \bar{\mathbf{C}}(\mathbf{q},\dot{\mathbf{q}})\dot{\theta} + \bar{\mathbf{G}}(\mathbf{q}) = \mathbf{U}_1 \quad (8)$$

where,

$$\bar{\mathbf{M}}(\mathbf{q}) = \begin{bmatrix} \left(m_t + m_c \sin^2\theta\right) & -m_c \sin\theta \\ -m_c \sin\theta & \left(m_c + m_l\right) \end{bmatrix};\ \mathbf{B} = \begin{bmatrix} b_t & 0 \\ 0 & b_r \end{bmatrix};$$

$$\bar{\mathbf{C}}(\mathbf{q},\dot{\mathbf{q}}) = \begin{bmatrix} m_c l \sin\theta\dot{\theta} \\ -m_c l\dot{\theta} \end{bmatrix};\ \bar{\mathbf{G}}(\mathbf{q}) = \begin{bmatrix} m_c g \sin\theta\cos\theta \\ -m_c g\cos\theta \end{bmatrix};$$

$$\mathbf{U}_1 = \begin{bmatrix} u_t \\ u_l \end{bmatrix};$$

Equation (8) can be represented into reduced order dynamics

$$\bar{\mathbf{M}}(\mathbf{q})\ddot{\mathbf{q}}_1 + \mathbf{B}\dot{\mathbf{q}}_1 + \bar{\mathbf{G}}(\mathbf{q}) = \mathbf{U} \quad (9)$$

where, $\mathbf{U} = \mathbf{U}_1 - \bar{\mathbf{C}}(\mathbf{q},\dot{\mathbf{q}})\dot{\theta}.$ (10)

The matrix differential Equation (9) describes reduced-order dynamics of the overhead crane. The mathematical model governed by Equation (9) is used to design the sliding mode control scheme in the next section.

III. Design of Sliding Mode Controller

In this section, we propose a sliding mode controller that moves the trolley from an initial position to its destination as fast as possible. Simultaneously, cargo vibration must completely vanish when the trolley arrives at the desired destination. Assume that all state variables are measurable. The design of the sliding mode controller is composed of two phases. First, we design a sliding surface in which the state trajectories restricted to that surface has the desired system behavior. Second, we design a control scheme in which the system is stable on the sliding surface. For this system, the switching surface is proposed that the actuated states $\mathbf{q}_1 = \begin{bmatrix} x & l \end{bmatrix}^T$ must come to desired constant values $\mathbf{q}_{1d} = \begin{bmatrix} x_d & l_d \end{bmatrix}^T$ and the cargo swing angle vanishes; this means un-actuated parameter θ approaches $\theta_d = 0$. Let us define tracking error vectors

$$\mathbf{e}_1 = \begin{bmatrix} x - x_d & l - l_d \end{bmatrix};\ e_2 = \theta - \theta_d = \theta \quad (11)$$

Next, let us define a sliding surface as a linear combination of position and velocity errors

$$\mathbf{s} = \begin{bmatrix} s_1 & s_2 \end{bmatrix}^{\mathrm{T}} = \dot{\mathbf{e}}_1 + \boldsymbol{\lambda}\mathbf{e}_1 + \boldsymbol{\alpha}e_2 \quad (12)$$

where, $\boldsymbol{\lambda}$ and $\boldsymbol{\alpha}$ are the design parameters determined by $\boldsymbol{\lambda} = \mathrm{diag}(\lambda_1, \lambda_2)$ and $\boldsymbol{\alpha} = \begin{bmatrix} \alpha_1 & 0 \end{bmatrix}^T$.

Differentiating the sliding surface **s** with respect to time leads to

$$\dot{\mathbf{s}} = \ddot{\mathbf{q}}_1 + \boldsymbol{\lambda}\dot{\mathbf{q}}_1 + \boldsymbol{\alpha}\dot{\theta} \quad (13)$$

After designing a sliding surface, we construct a feedback controller. Matrix $\bar{\mathbf{M}}(\mathbf{q})$ is positive definite for every $l > 0$ and $\theta < \pi/2$. Equation (9) can be rewritten as

$$\ddot{\mathbf{q}}_1 = \bar{\mathbf{M}}^{-1}(\mathbf{q})\left(\mathbf{U} - \mathbf{B}\dot{\mathbf{q}}_1 - \bar{\mathbf{G}}(\mathbf{q})\right) \quad (14)$$

Substituting Equation (14) to Equation (13) and setting $\dot{\mathbf{s}} = \mathbf{0}$, we obtain

$$\mathbf{U} = \left(\mathbf{B} - \bar{\mathbf{M}}(\mathbf{q})\boldsymbol{\lambda}\right)\dot{\mathbf{q}}_1 - \bar{\mathbf{M}}(\mathbf{q})\boldsymbol{\alpha}\dot{\theta} + \bar{\mathbf{G}}(\mathbf{q}) \quad (15)$$

The matrix Equation (4) does not completely describe system behavior; it is just an approximation. Therefore, an approximated control law where $\dot{\mathbf{s}} = \mathbf{0}$ can be presented as

$$\hat{\mathbf{U}} = \left(\mathbf{B} - \bar{\mathbf{M}}(\mathbf{q})\boldsymbol{\lambda}\right)\dot{\mathbf{q}}_1 - \bar{\mathbf{M}}(\mathbf{q})\boldsymbol{\alpha}\dot{\theta} + \bar{\mathbf{G}}(\mathbf{q}) \quad (16)$$

Furthermore, to maintain the state trajectory of the system on the sliding surface, we must introduce the switching action as

$$\mathbf{U}_{sw} = -\mathbf{K}\mathbf{sign}(\mathbf{s}) \quad (17)$$

Therefore, the overall sliding mode control law composed of approximated control and switching action can be written as

$$\begin{aligned} \mathbf{U} &= \hat{\mathbf{U}} + \mathbf{U}_{\mathrm{sw}} \\ &= \left(\mathbf{B} - \bar{\mathbf{M}}(\mathbf{q})\boldsymbol{\lambda}\right)\dot{\mathbf{q}}_1 - \bar{\mathbf{M}}(\mathbf{q})\boldsymbol{\alpha}\dot{\theta} + \bar{\mathbf{G}}(\mathbf{q}) - \mathbf{K}\mathbf{sign}(\mathbf{s}) \end{aligned} \quad (18)$$

where, $\boldsymbol{\lambda}$ is a 2x2 constant matrix, $\boldsymbol{\alpha}$ is a 2x1 constant matrix, and $\mathbf{K} = \mathrm{diag}(K_1, K_2)$. The design parameters $\boldsymbol{\lambda}$, $\boldsymbol{\alpha}$, and **K** are chosen so that **s** approaches zero as fast as possible. $\hat{\mathbf{U}}$ is used for low-frequency control action. Conversely, $\mathbf{U}_{sw}$ corresponds to high-frequency control. $\mathbf{sign}(\mathbf{s})$ is a sign function whose *i*-th component has form

$$\left[\mathbf{sign}(\mathbf{s})\right]_i = \begin{cases} +1 \text{ if } s_i > 0 \\ 0 \text{ if } s_i = 0 \\ -1 \text{ if } s_i < 0 \end{cases} \quad (19)$$

However, a switching control usually causes chattering of state trajectory around the switching surface. To reduce chattering, we replace the **sign**(**s**) function by a saturation function as follows

$$\mathbf{U}_{sw} = -\mathbf{K}\mathbf{sat}(\mathbf{s}) \quad (20)$$

where,

$$\left[\mathbf{sat}(\mathbf{s})\right]_i = \begin{cases} 1 \text{ if } s_i/\varepsilon > 1 \\ s_i/\varepsilon \text{ if } -1 < s_i/\varepsilon < 1 \\ 1 \text{ if } s_i/\varepsilon < -1 \end{cases} \quad (21)$$

And ε is a constant denoted thickness of boundary layer.

IV. System Stability

In this section, we find constraint conditions to make the system stable. The design of a sliding mode controller is composed of determining a sliding surface and designing a switched control. The sliding surface is chosen so that the state trajectories are attracted to this surface and the switched control action (17) must guarantee the stability of system states on the sliding surface. In other words, the sliding mode control scheme (18) guarantees that all state trajectories reach the sliding surface (reaching condition) and slide into the desired values on this surface. The reaching condition [13] is determined by considering the Lyapunov function $V = 0.5\mathbf{s}^T\mathbf{s}$ such that

$$\dot{V} = \mathbf{s}^T\dot{\mathbf{s}} \le -\boldsymbol{\eta}|\mathbf{s}| \quad (22)$$

where, $\boldsymbol{\eta} = \text{diag}(\eta_1, \eta_1)$ is a positive matrix. The switched gain $\mathbf{K} = \text{diag}(K_1, K_2)$ of the sliding mode control (18) is chosen so that the reaching condition is satisfied. Substituting (13), (14), and (18) into (22) and simplifying leads to

$$\dot{V} = -\mathbf{s}^T\bar{\mathbf{M}}^{-1}(\mathbf{q})\mathbf{K}\mathbf{sign}(\mathbf{s}) = -\bar{\mathbf{M}}^{-1}(\mathbf{q})\mathbf{K}|\mathbf{s}| \quad (23)$$

$\bar{\mathbf{M}}(\mathbf{q})$ is positive definite for every $l > 0$ and $\theta < \pi/2$. Therefore, $\dot{V} = -\bar{\mathbf{M}}^{-1}(\mathbf{q})\mathbf{K}|\mathbf{s}| < 0$ for every positive definite $\mathbf{K}$. The sliding surface $\mathbf{s}$ approaches zero as t tends to infinity for every $K_1 > 0$ and $K_2 > 0$. Comparing between expressions (22) and (23), $\mathbf{K}$ can be determined as

$$\mathbf{K} = \boldsymbol{\eta}\bar{\mathbf{M}}(\mathbf{q})\big|_{\theta\to 0} = \begin{bmatrix} \eta_1 & 0 \\ 0 & \eta_2 \end{bmatrix}\begin{bmatrix} m_t & 0 \\ 0 & m_c + m_l \end{bmatrix}$$

which implies that

$$K_1 = \eta_1 m_t;\ K_2 = \eta_2(m_c + m_l) \quad (24)$$

Hence, reaching condition (24) guarantees the stability of the sliding surface. More precisely, if the switching gain $\mathbf{K}$ is chosen according to Equation (24), the control forces (18) drive the state trajectories $\mathbf{q} = [\mathbf{q}_1 \quad \theta]^T$ to the sliding surface. However, the sliding mode control scheme (18) does not ensure that these states approach the desired values on the sliding surface. Therefore, we prove that the crane system is stabilized on the surface under given conditions by analyzing the un-actuated dynamics (5) and the switching manifold (12). Thus, Equation (5) can be rewritten as

$$\ddot{\theta} = \mathbf{A}_1\ddot{\mathbf{q}}_1 - \mathbf{B}_1\dot{\mathbf{q}}_1 - \mathrm{C}_1 \quad (25)$$

where,

$$\mathbf{A}_1 = [\cos\theta/l \quad 0];\ \mathbf{B}_1 = [0 \quad 2\dot{\theta}/l];\ \mathrm{C}_1 = g\sin\theta/l$$

Substituting (14) to (25) leads to

$$\ddot{\theta} = \bar{\mathbf{M}}^{-1}(\mathbf{q})\mathbf{A}_1\left(\mathbf{U} - \mathbf{B}\dot{\mathbf{q}}_1 - \bar{\mathbf{G}}(\mathbf{q})\right) - \mathbf{B}_1\dot{\mathbf{q}}_1 - \mathrm{C}_1 \quad (26)$$

By substituting (15) to (26), we obtain

$$\ddot{\theta} = -(\mathbf{A}_1\boldsymbol{\lambda} + \mathbf{B}_1)\dot{\mathbf{q}}_1 - \mathbf{A}_1\boldsymbol{\alpha}\dot{\theta} - \mathrm{C}_1 \quad (27)$$

From the sliding surface Equation (12) $\mathbf{s} = \mathbf{0}$ we obtain

$$\mathbf{s} = \dot{\mathbf{q}}_1 + \boldsymbol{\lambda}(\mathbf{q}_1 - \mathbf{q}_{1\mathrm{d}}) + \boldsymbol{\alpha}\theta = \mathbf{0}$$

which is equivalent to

$$\dot{\mathbf{q}}_1 = -\boldsymbol{\lambda}(\mathbf{q}_1 - \mathbf{q}_{1\mathrm{d}}) - \boldsymbol{\alpha}\theta \quad (28)$$

Let us define

$$\mathbf{z} = [z_1 \quad z_2 \quad \mathbf{z}_3]^T = [\theta \quad \dot{\theta} \quad \mathbf{q}_1 - \mathbf{q}_{1d}]^T$$

Note that $\mathbf{z} \in R^4$. Equations (27) and (28) become

$$\dot{z}_2 = -(\mathbf{A}_1\boldsymbol{\lambda} + \mathbf{B}_1)\dot{\mathbf{z}}_3 - \mathbf{A}_1\boldsymbol{\alpha}z_2 - \mathrm{C}_1 \quad (29)$$

$$\dot{\mathbf{z}}_3 = -\boldsymbol{\alpha}z_1 - \boldsymbol{\lambda}\mathbf{z}_3 \quad (30)$$

Substituting (30) to (29) leads to

$$\dot{z}_2 = \begin{pmatrix} (\mathbf{A}_1\boldsymbol{\lambda} + \mathbf{B}_1)\boldsymbol{\alpha}z_1 - \mathbf{A}_1\boldsymbol{\alpha}z_2 \\ +(\mathbf{A}_1\boldsymbol{\lambda} + \mathbf{B}_1)\boldsymbol{\lambda}\mathbf{z}_3 - \mathrm{C}_1 \end{pmatrix} = h(\mathbf{z}) \quad (31)$$

Combining Equations (31) and (30) with $\dot{z}_1 = z_2$ can be represented in matrix form

$$\begin{bmatrix} \dot{z}_1 \\ \dot{z}_2 \\ \dot{\mathbf{z}}_3 \end{bmatrix} = \begin{bmatrix} z_2 \\ \begin{pmatrix} (\mathbf{A}_1\boldsymbol{\lambda} + \mathbf{B}_1)\boldsymbol{\alpha}z_1 - \mathbf{A}_1\boldsymbol{\alpha}z_2 \\ +(\mathbf{A}_1\boldsymbol{\lambda} + \mathbf{B}_1)\boldsymbol{\lambda}\mathbf{z}_3 - \mathrm{C}_1 \end{pmatrix} \\ -\boldsymbol{\alpha}z_1 - \boldsymbol{\lambda}\mathbf{z}_3 \end{bmatrix} \quad (32)$$

Linearization (32) about the equilibrium position $\mathbf{z} = \mathbf{0}$ (or $\mathbf{q} = \mathbf{q}_d$) can be rewritten into a linearized form

$$\begin{bmatrix} \dot{z}_1 \\ \dot{z}_2 \\ \dot{\mathbf{z}}_3 \end{bmatrix} = \begin{bmatrix} 0 & 1 & \mathbf{0}_{1\times 2} \\ \dfrac{\partial h(\mathbf{z})}{\partial z_1}\Big|_{\mathbf{z}=\mathbf{0}} & \dfrac{\partial h(\mathbf{z})}{\partial z_2}\Big|_{\mathbf{z}=\mathbf{0}} & \dfrac{\partial h(\mathbf{z})}{\partial \mathbf{z}_3}\Big|_{\mathbf{z}=\mathbf{0}} \\ -\boldsymbol{\alpha} & \mathbf{0}_{2\times 1} & -\boldsymbol{\lambda} \end{bmatrix}\begin{bmatrix} z_1 \\ z_2 \\ \mathbf{z}_3 \end{bmatrix}$$

Or

$$\dot{\mathbf{z}} = \mathbf{A}\mathbf{z} \quad (33)$$

where,

$$\frac{\partial h(\mathbf{z})}{\partial z_1}\Big|_{\mathbf{z}=\mathbf{0}} = (\mathbf{A}_1\boldsymbol{\lambda} + \mathbf{B}_1)\boldsymbol{\alpha}\big|_{\mathbf{q}=\mathbf{q}_d} = \frac{\lambda_1\alpha_1}{l_d}$$

$$\left.\frac{\partial h(\mathbf{z})}{\partial z_2}\right|_{\mathbf{z}=\mathbf{0}} = -\mathbf{A}_1\boldsymbol{\alpha}\big|_{\mathbf{q}=\mathbf{q}_d} = -\frac{\alpha_1}{l_d}$$

$$\left.\frac{\partial h(\mathbf{z})}{\partial \mathbf{z}_3}\right|_{\mathbf{z}=\mathbf{0}} = (\mathbf{A}_1\boldsymbol{\lambda}+\mathbf{B}_1)\boldsymbol{\lambda}\big|_{\mathbf{q}=\mathbf{q}_d} = \begin{bmatrix}\frac{\lambda_1^2}{l_d} & 0\end{bmatrix}$$

thus

$$\mathbf{A} = \begin{bmatrix} 0 & 1 & 0 & 0 \\ \frac{\lambda_1\alpha_1}{l_d} & -\frac{\alpha_1}{l_d} & \frac{\lambda_1^2}{l_d} & 0 \\ -\alpha_1 & 0 & -\lambda_1 & 0 \\ 0 & 0 & 0 & -\lambda_2 \end{bmatrix} \tag{34}$$

The system dynamics (33) is stable if and only if all eigenvalues of **A** lie in the right-half s-plane. We find the conditions for system stability by Routh's criterion. The linearized system (33) is stable if and only if all coefficients of the characteristic polynomial of **A** are positive, and all terms in the first column of Routh's table have positive signs. From these requirements and after some calculations, we obtain

$$\left(\frac{\alpha_1}{l_d}+\lambda_1+\lambda_2\right)>0;\left(\frac{\alpha_1}{l_d}+\lambda_1\right)\lambda_2>0 \tag{35}$$

In summary, the sliding mode control controller (18) stabilizes the crane system described by Equation (4) if sufficient conditions (35) are guaranteed. The selection of parameters of the sliding mode controller must satisfy the given conditions (35).

V. Simulation and Experiment

To obtain system responses, we simulate the system dynamics (4) taken by the sliding mode control forces (18) based on a MATLAB environment. The overhead crane system is simulated in two cases as

Case 1: m_c = 0.85 kg; m_t = 5 kg; m_l = 2 kg; b_t = 20 N.m/s; b_r = 50 N.m/s; g = 9.81 m/s^2; λ_1 = 0.9; λ_2 = 1.2; α_1 = 2.5; ε = 0.05. The chosen design parameters must satisfy the conditions (35).

Case 2: An overhead crane is an under-actuated system with uncertain components. For this system, m_c and $\mathbf{b}$ = [b_t b_r] are considered uncertain components. The variations of uncertainties depend on each particular operation, working condition, and environment. To verify the robustness of the proposed controller, we simulate this system in case of value varying of uncertain components: Δm_c =+400%, $\Delta\mathbf{b}$=[–20% –20%] and the remaining the design parameters as Case 1.

We also select $\boldsymbol{\eta}=\text{diag}(40,35)$ for Case 1 and $\boldsymbol{\eta}=\text{diag}(40,18.5)$ for Case 2. The different selection of $\boldsymbol{\eta}$ is to retain switched gain $\mathbf{K}=\text{diag}(200,100)$ for both cases.

For both cases, the cargo is handled on the cable with an initial length l_0 = 0.1 m, and the cable is initially perpendicular to the ground ($\theta_0 = 0^0$). The control inputs (18) must be created so that the cargo is lowered to 0.4 m, the desired cable length; and the trolley moves 0.3 m, the desired displacement ($l_d = 0.4$, $x_d = 0.3$). Lowering the cargo and moving the trolley must be started at the same initial time. The simulation results are presented in Fig. 3 to Fig. 11.

Figure 2. An overhead crane system for experiment

Furthermore, to verify the quality of simulation based responses, an experimental study is carried out with the realistic overhead crane system (Fig. 2). The crane system consists of two DC motors that drive the trolley and hoist the cargo. Three incremental encoders measure the trolley displacement, cargo hoisting, and cargo swing. The real-time crane system is controlled by hoist PC based on the MATLAB and SIMULINK environments with xPC Target solution. In this system, we use two interfacing cards attached to the target PC. One is the NI PCI 6025E multifunction card, which is used to send the direction control signals to the motor amplifiers. The other is the NI PCI 6602 card, used to acquire the pulse signals from the encoders and send PWM signals to the amplifiers. The experimental results are described in Figs. 6–8.

Fig. 3 describes sliding surfaces in two simulated cases. The sliding surfaces reach 0 within a considerably short time. The motion of the system states includes two phases. First, state trajectories reach the switching surface, and second, they slide to desired values on this surface. The first phase is sensitive and the second phase is insensitive to parameter variations [14]. Therefore, the less the reaching time of the switching surface, the more robust the system. The design parameters must be chosen so that the reaching time of the sliding surface is as short as possible. The sliding surface s_1 is related to trolley displacement and cargo swing angle and the sliding surface s_2 has the relationship with cargo hoisting motion. The sliding surface s_1 almost all retain its shape in both cases. Therefore, the responses of trolley motion and cargo swing are not varied obviously when the simulation is changed from Case 1 to Case 2 (Figs. 6–7). Meanwhile, the sliding surface s_2 of Case 1 reach to zero faster than that of Case 2. Hence, the cargo lowering of Case 1 is faster than that of Case 2 (Figs. 8, 11).

Control signals, u_t and u_l, are respectively represented in Fig. 4 and Fig. 5. Clearly, these forces approach constant values as system outputs reach the reference values. For example, Fig. 4 shows that the driving forces of the trolley arrive at 0 after 4.5 seconds for both simulation cases. In Case 1, the lifting force of cargo, u_l, presented in Fig. 5, tends to the value, $u_l = -m_c g = -0.85 \times 9.81 = -8.34$ (N), when the cargo is lowered down the 0.4 m cable length after 5.5 seconds (see Fig. 8). The minus sign of the lifting force implies that its direction is opposite that of the cargo weight. Clearly, at steady state, the lifting force is equal to the gravitational force of the cargo that the cargo remains balanced on the cable. Similarly in Case 2, Fig. 5 shows that the lifting force u_l and the gravitational force of the cargo are equal but opposite in direction ($u_l = -m_c g = -3.4 \times 9.81 = -33.35$ N) at steady state.

The cargo sway responses are illustrated on Fig. 6. The simulated responses completely vanished after one oscillation period. Meanwhile, the experimental curve reaches to steady-state after more than two periods. However, the setting time of simulated responses relatively equal to that of experimental one, $t_s \approx 4$ s. The trajectories of cargo also show that the cargo swing is kept small during the transfer process: $\theta_{\max} = 4.173^0$ for simulation case and $\theta_{\max} = 2.637^0$ for experimental one.

Fig. 7 represents the responses of trolley travelling for both simulation and experiment. These responses asymptotically approach to desired values with the different setting time. For example, t_s = 4.5 s for simulated responses and t_s = 5.5 s for experimental curve. Similarly, the cargo lowering responses are shown on Fig. 8. It seems that both simulation and experiment responses do not have maximum overshoot. These responses achieve the steady-state after the same setting time, t_s =5.5 s.

The swing velocity of the cargo, the velocity of the trolley, and the lowering velocity of the cargo are respectively expressed in Fig. 9, Fig. 10, and Fig. 11. Although they are not the outputs that need to be controlled, they remain state trajectories of the system. The transient period of these system responses can be divided into two phases: the acceleration and deceleration phases. For example, the trolley accelerates in the first 0.8 seconds and then decelerates in the remaining 3.7 seconds (Fig. 10). The cargo is rapidly hoisted during the first 0.3 seconds, with speed slowing down during the remaining 5.2 seconds (Fig. 11).

Fig. 3 to Fig. 11 in simulation case 2 show that the surfaces approach 0 and all state trajectories asymptotically reach the desired values after a finite time despite widely varying uncertainties. Hence, we can conclude that the proposed siding mode controller is robust and insensitive even if the overhead crane is an un-actuated system with wide parameter variations.

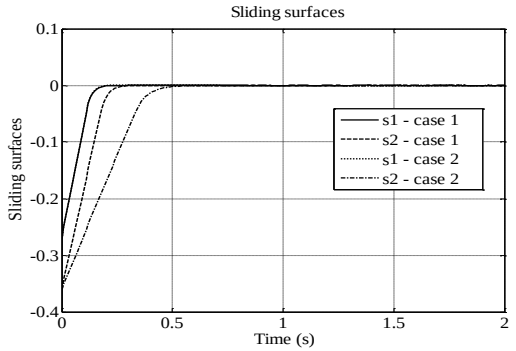

Figure 3. Sliding surfaces

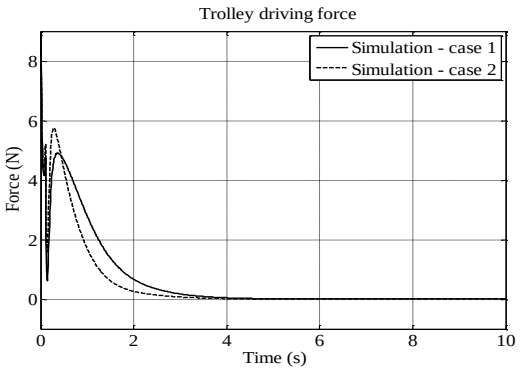

Figure 4. Trolley driving force

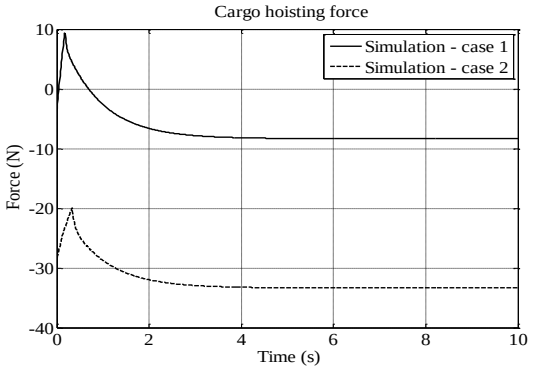

Figure 5. Cargo lifting force

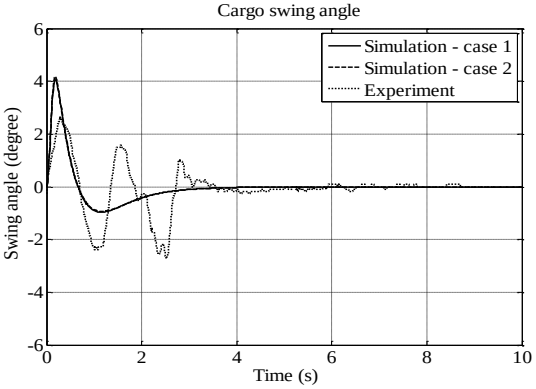

Figure 6. Cargo swing angle

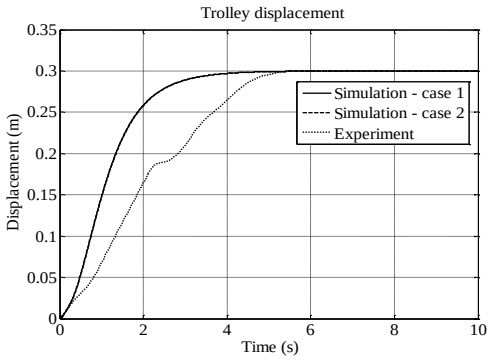

Figure 7. Trolley displacement

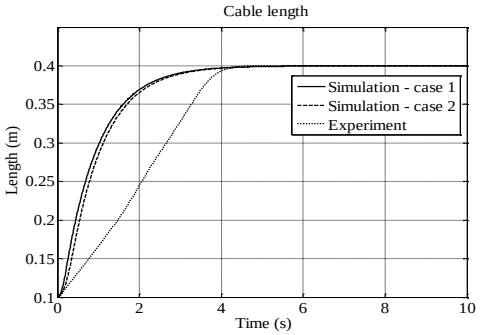

Figure 8. Cargo lowering motion

To show the improvement of proposed controller, the comparison of system behavior with study [3] is shown in Table 1. Both SMC responses and feedback linearization (FL) responses [3] converge to desired values without steady-state errors. The settling times of SMC responses are shorter than those of FL responses. However, FL cargo swing angle [3] is smaller than SMC one.

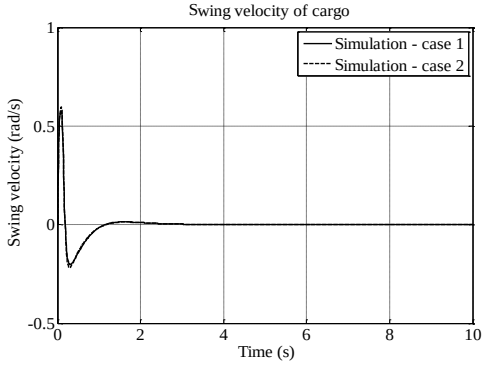

Figure 9. Cargo swing velocity

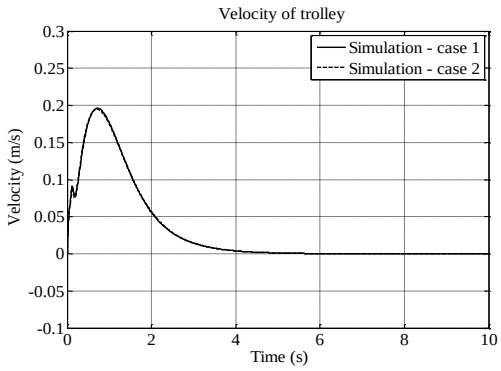

Figure 10. Trolley velocity

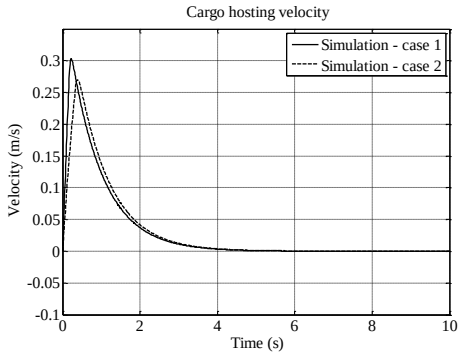

Figure 11. Cargo lowering velocity

VI. Conclusion

In this study, we successfully designed a sliding mode controller for a complicated operation of an overhead crane: simultaneously combining control of cargo lifting, trolley moving, and cargo swing vanishing. From the simulation and experiment results, all system responses are asymptotically stable: cargo swing completely vanished and trolley motion and cargo lifting/lowering accurately reached the reference values. Furthermore, the proposed controller stabilized the crane system even if the overhead crane is an under-actuated system with a wide range of varying uncertainties. For the next research, we will enhance this sliding mode control problem for 3D overhead cranes.

References

[1] T. Erneux and T. K. Nagy, "Nonlinear stability of a delayed feedback controlled container crane," *Journal of Vibration and Control*, no. 13, pp. 603-616, 2007.

[2] C. C. Cheng and C. Y. Chen, "Controller design for an overhead crane system with uncertainty," *Control Engineering Practice* 4, pp. 645-653, 1996.

[3] T. A. Le, G. H. Kim, M. Y. Kim, and S. G. Lee, "Partial feedback linearization control of overhead cranes with varying cable lengths," *International Journal of Precision Engineering and Manufacturing*, no. 13, pp. 501-507, 2012.

[4] J. Yi, N. Yubazaki, and K. Hirota, "Anti-swing and positioning control of overhead traveling crane," *Information Sciences*, no. 155, pp. 19-42, 2003.

[5] S. K. Cho and H. H. Lee, "A fuzzy-logic anti-swing controller for three dimensional overhead cranes," *ISA Transactions*, no. 41, pp. 235-243, 2002.

[6] R. Toxqui, W. Yu, and X. Li, "Anti-swing control for overhead crane with neural compensation," in *Proc. International Joint Conference on Neural Networks*, Vancouver, Canada, 2006.

[7] H. H. Lee, Y. Liang, and D. Segura, "A sliding mode anti-swing trajectory control for overhead cranes with high speed load hoisting," *Journal of Dynamic Systems, Measurements, and Control*, vol. 128, pp. 842-845, 2006.

[8] K. K. Shyu, C. L. Jen, and L. J. Shang, "Design of sliding mode control for anti-swing control of overhead cranes," in *Proc. 31st Annual Conference of IEEE Industrial Electronics Society*, RC, USA, 2005.

[9] K. K. Shyu, C. L. Jen, and L. J. Shang, "Sliding mode control for an under-actuated overhead crane system," in *Proc. 32th Annual Conference of IEEE Industrial Electronics Society*, Paris, France, 2006.

[10] N. B. Almutairi and M. Zribi, "Sliding mode control of a three-dimensional overhead crane," *Journal of Vibration and Control*, no. 15, pp. 1679-1730, 2009.

[11] D. Liu, J. Yi, D. Zhao, and W. Wang, "Adaptive sliding mode fuzzy control for a two dimensional overhead crane," *Mechatronics*, no. 15, pp. 505-522, 2004.
[12] Bartolini, N. Orani, A. Pisano, and E. Usai, "Load swing damping in overhead cranes by sliding mode technique," in *Proc. 39th IEEE Conference on Decision and Control*, Australia, 2000.
[13] J. J. E. Slotine and W. Li, *Applied Nonlinear Control*, Prentice Hall, Englewood Cliffs, NJ, 1991.
[14] S. G. Sajad and B. H. Mohammad, "Optimal design of rotating sliding surface for sliding mode control," in *Proc. American Control Conference*, Missouri, USA, 2009.

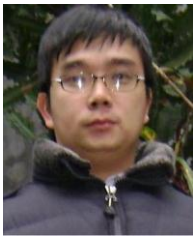

Le Anh Tuan graduated both B. Eng. and M. Eng. in Mechanical Engineering and Marine Machinery from Vietnam Maritime University in 2003 and 2007, respectively. He received the Ph.D. degree in Mechanical Engineering from Kyung Hee University, South Korea in 2012. Currently, he is an assistant professor in Mechanical Engineering of Vietnam Maritime University. Dr. Tuan is also a faculty of Duy Tan University, Da Nang, Vietnam. His interested research composes of applied nonlinear control, dynamics and control of industrial machines.